

## Wind Turbine Airfoil Performance Optimization using the Vortex Lattice Method and a Genetic Algorithm

Christoph Burger and Roy Hartfield  
Aerospace Engineering, Auburn University

### Abstract

This paper examines the viability of using the combination of the vortex lattice method for aerodynamic performance prediction with a genetic algorithm for the optimization of the aerodynamic performance of horizontal axis wind turbine blades. The work described in this paper includes the adaptation of a vortex lattice code designed to predict propeller performance to wind turbine performance prediction and the optimization process including results for both single point and multipoint design optimization efforts.

### Background

The economics of deploying large wind turbine farms as a substantial source of electrical power is driven in large part by the efficiency of power conversion from wind energy to rotational mechanical energy. In the 1920's, Betz formulated the basic analysis for the limiting case for horizontal axis wind turbine efficiency and set up the guidelines for how windturbine efficiencies should be calculated. A modern explanation of the Betz analysis can be found in Reference 1. In the 1930's Glauert applied classical aerodynamic methods to airplane propeller designs in an effort to optimize performance of the horizontal axis machine for propulsion.<sup>2</sup> In the 1970's and 1980's blade element and momentum theory models were developed and refined for modeling wind turbine performance<sup>3-5</sup> and the efficiency of these models made them ideally suited for the genetic algorithm optimization work performed in the 1990's by Selig et al.<sup>6</sup> This method for optimizing horizontal axis wind turbines using genetic algorithms used an improved version of the momentum theory models and demonstrated a successful and efficient optimization strategy. Hampsey<sup>1</sup> improved upon the optimization efforts by using a B-spline approach for modeling the blades along with a panel method for performance prediction. In this important optimization using a relatively higher order method for aerodynamic prediction, the blade geometries were not modeled using traditional airfoil shape theory.

In the development of performance prediction for sails, it has been shown that the prediction of aerodynamic loads using the vortex lattice method is often much more accurate than load predictions based on simpler momentum theory methods. As with the panel methods, computational efficiency necessary for optimization can be maintained with the vortex lattice method.<sup>7</sup> A vortex lattice method has been applied to ship propellers<sup>8</sup> and to airplane propellers and has been shown to accurately predict performance in appropriate applications.<sup>9,10</sup> The airplane propeller analysis reported in

Ref. 9 has been adapted as the primary engine for horizontal axis wind turbine performance in this effort.

The genetic algorithm(GA) used in this effort is the Improve© Code developed and implemented in several aerospace applications by Anderson.<sup>11,12</sup> This code uses a tournament based method for reproduction and has options for elitism and pareto development of multiple goal problems. The GA and vortex lattice wind turbine model have been used to optimize the aerodynamic performance of wind turbines for power density for a single operating condition and for different wind speeds at a constant angular velocity as described by the Weibull distribution with a shape factor of 2.

### Vortex Lattice Method

Even though the vortex lattice theory does not include any viscous or compressibility effects, *Richard Shiu Wing Cheung*<sup>10</sup> proved that aircraft propeller performance predictions can be close to experimental performance data. He also showed that the inclusion of 2-D drag data results in only a minor improvement with respect to experimental data. Depending on the thickness of the propeller airfoil, the vortex lattice method of lifting surface with one or two layers has to be chosen. In this paper only wind turbines with thin airfoils are investigated. Thus the vortex lattice method of lifting surface with a single layer of vortex elements is used for all numerical propeller performance predictions.

### Airfoil Performance Program

#### Basic Geometry

The basic geometric shape assumed for the wind turbine blades is a swept wing design with swept wing with a chord length that decreases linearly with radial position. The geometric flexibility of the blades includes blade length, blade width at the root and tip, blade sweep, and blade angle of attack as a function of radial position. A set of parameters is chosen to describe the blade planform. The blade is then designed by choosing a design operating speed and a free stream wind velocity. The blade shape is then set so that the blade slices through the stream without altering the free stream momentum. An angle of attack is then added to the blade using a distribution function.

A schematic of the blade planform illustrating the profile and sweep is shown in Figure 1.

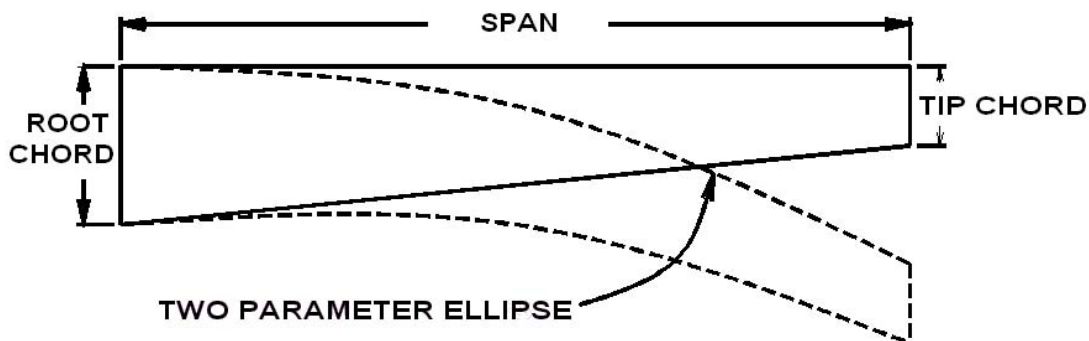


Figure 1: Schematic of blade planform.

Two different functions describing the angle of attack distribution for the blades were investigated. An elliptic distribution which allows for angles of attack ranging from nearly constant functions to fully elliptic profiles was investigated because this class of functions is known to produce desirable distributions for angle of attack on aircraft wings. This functional development is described more fully in Ref. 9. After looking at the results of the wake with this distribution, a parabolic profile for the angle of attack distribution was investigated. The parabolic profile was instituted in the form of a square root function as shown in equation 1.

$$aoa = aoax\sqrt{aoah - y} + aoay \quad (1)$$

Here,  $aoa$  is the angle of attack at span location  $y$ , and  $aoax$ ,  $aoah$ , and  $aoay$  are free constants. The one additional parameter to fully describe the blade shape is the chordwise position of the center of rotation. For multiple advance ratios, an additional parameter is included to allow for the fixed geometry blade to change the total pitch angle to better accommodate the off design advance ratios.

Depending on the parameters selected, the propeller blade shape can vary from a simple straight blade propeller to a swept back blade with a linear chord length distribution with either an elliptic or a parabolic angle of attack distribution.

### **Airfoil Generation**

In the airfoil generation process all NACA 4-digit series airfoils can be created. The GA input parameters which determine the airfoil type are;

- max camber
- position of max camber

Since the airfoil performance program uses only a single lifting surface layer of vortex elements the thickness is not taken into account. To get close data to experimental results the program applies only to thin airfoil sections as shown by *Richard Shiu Wing Cheung*<sup>10</sup>. After the airfoil is selected, the mean line is determined by taking the average value of the upper and lower airfoil surface. This mean line describes the lifting surface of vortex elements for the air foils. The airfoil characteristics including max camber and position of the max camber are constant over the entire air foil span.

### **Airfoil Performance**

The air foil performance program consists of several components which generate the turbine blade geometry, grid discretization, influence coefficient determination and Gauss solver subroutine to solve for the unknown vortex strength.

To allow parameters to change during the optimization, an input file which contains the airfoil design variables is read in by the program. Other fixed parameters such as the free stream velocity, rotational speed, number of panels, impeller hub diameter and air density, are set at the beginning of the program. Besides the integration into the GA, the airfoil performance program can also be used to determine the performance of a wind turbine impeller over a range of upwind speed conditions.

### **Grid Generation**

The air foils are divided up into chordwise and spanwise panels. A single panel side is defined by two following nodal points. A quadrilateral element is constructed from two neighboring spanwise and chordwise vortex elements. Control points are located

in the center of the quadrilateral elements. The control points are where the influence of the individual vortex elements is evaluated. The number of panel elements can be set in the variable definition section of the program, which is fixed throughout the optimization. In the spanwise direction the location of the grid points follows James.<sup>13</sup> Thus the discretization has equidistance between the nodal points with the tip element moved one quarter interval inward to account for the wingtip vortex. See also Ref. 8 for more detailed description of panel distribution functions. In the chordwise direction the panels are divided up into even spacing.

### Quadrilateral and Horseshoe Elements

The panel elements consist of four straight vortex lines which form a quadrilateral. To fulfill Lord Kelvin's theorem the circulation along the panel sides is constant. More detail on that constraint is found in Refs. 14 and 15.

The wake of the propeller is simulated by horseshoe vortices which extend from the last chordwise panel two revolutions downstream. The pitch of the horseshoe elements is constant, which coincide with Goldstein's helical vortex model<sup>16</sup>, and follows the trailing edge panel to satisfy the Kutta condition. Slipstream contraction is neglected to simplify the geometry of the wake. See Figure 2 below.

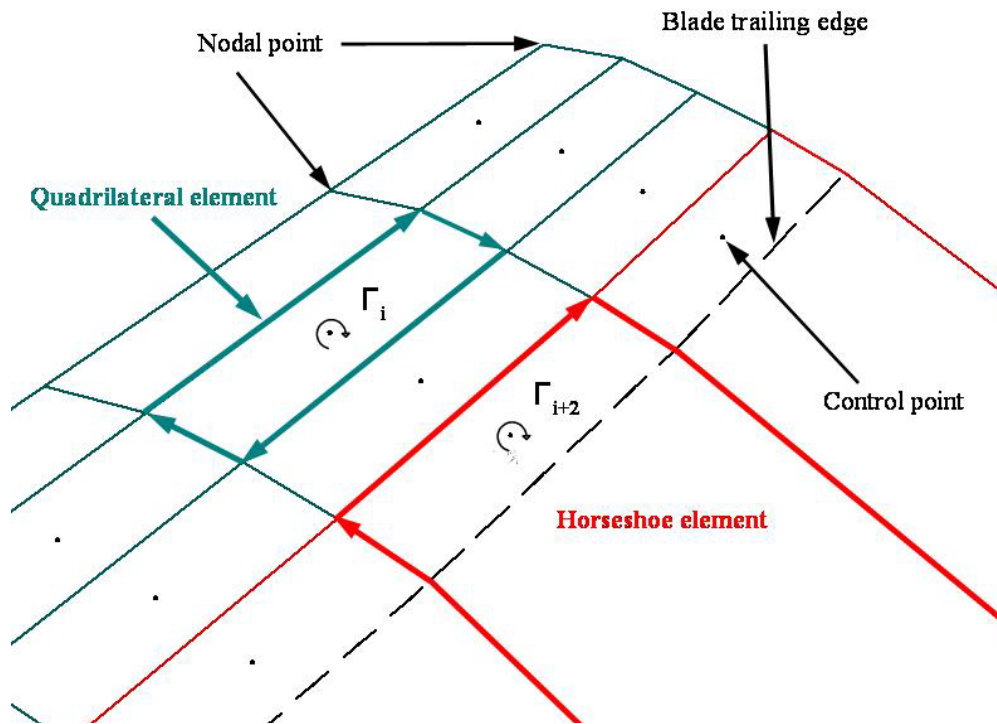


Figure 2: Blade discretization into quadrilateral and horseshoe elements

For the work presented here, compressibility modeling is not included and no viscous effects are accounted for. These phenomena will be incorporated in future modeling efforts; however, for the flow velocities of principle interest to this investigation compressibility and viscous effects do not significantly alter the results.

## Results

To gain some confidence in the prediction scheme, some comparisons with the calculations of other researchers are included in the optimization results. An inverse method for optimization was used in Reference 17, and results from this optimization are compared to results obtained for optimized blades using the vortex lattice method in Figure 3. The parameter of interest in this comparison is the efficiency. In all cases for this paper, the efficiency is defined as the power extracted by the wind turbine divided by the power in the upwind stream. The power produced by the wind turbine is calculated by calculating the torque applied to the machine due to the aerodynamic loading calculated using the vortex lattice method. This torque is multiplied by the operating speed to get shaft power. The power in the wind is the mass flow rate multiplied by the kinetic energy per unit mass.

All optimizations prepared for the present investigation involve maximizing power produced at the hub for a given wind speed, operating speed and blade length. The angle of attack distribution employed in this comparative work is described by the parabolic function. The diameter of the wind turbines compared in Figure 3 is 16 m and the operating speed is 120 rpm for all but one case. In all four of these cases, the machines are constructed with 2 blades. The geometry was not specified clearly enough in Ref. 17 to allow for a rigorous comparison of performance but the qualitative comparison is favorable considering that the wind turbines were optimized using different methods and different performance prediction schemes. There are several noteworthy characteristics of these results. Fundamentally, if the machine is optimized for power output at a given wind speed, the efficiency will peak at a slightly lower wind speed. Also, the Betz limit on this plot is approximately 60%. For the 120 rpm case, the peak efficiency of the two GA optimized machines bracket the performance of the machine analyzed in Ref. 17. Further investigation of the performance prediction routine is necessary but it would appear that a slight over prediction of performance is occurring at the lower wind speeds.

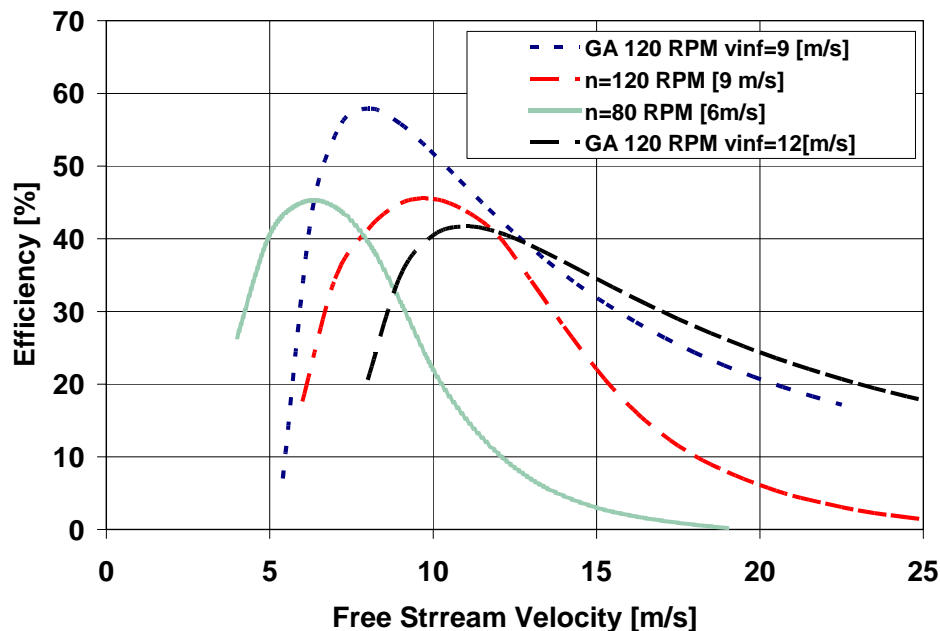


Figure 3: Comparison of blade efficiencies with other analyses

Additional verification and validation of the prediction tool using experimental data is imperative and is currently under way. However, the prediction tool is clearly providing realistic estimates of the wind turbine performance and can be used with confidence to at least qualitatively optimize wind machines.

To more clearly understand the details of the optimization efforts, the wake for the two cases discussed above is displayed in Figures 4 and 5. For clarity, the wake from only one of the two blades is shown in the plot. For the vortex lattice method employed in this work, the trailing legs for the horse shoe vortices are not “managed” in any special way. These legs are allowed to travel downstream for two full rotations at the angle at which they leave the trailing edge of the airfoil. The only constraint placed on the trailing legs is that they are required to travel downstream. This does not accurately portray the velocity field far away from the wind turbine since the free stream momentum would bend and stretch the trailing legs; however, the position of the trailing legs far down stream of the air foils appears to have little impact on the predicted torque with the primarily quadrilateral element version of the vortex lattice code employed here. For this reason, the wake plots shown here serve primarily to illustrate the profile of momentum exchange between the wind turbine blades and the free stream.

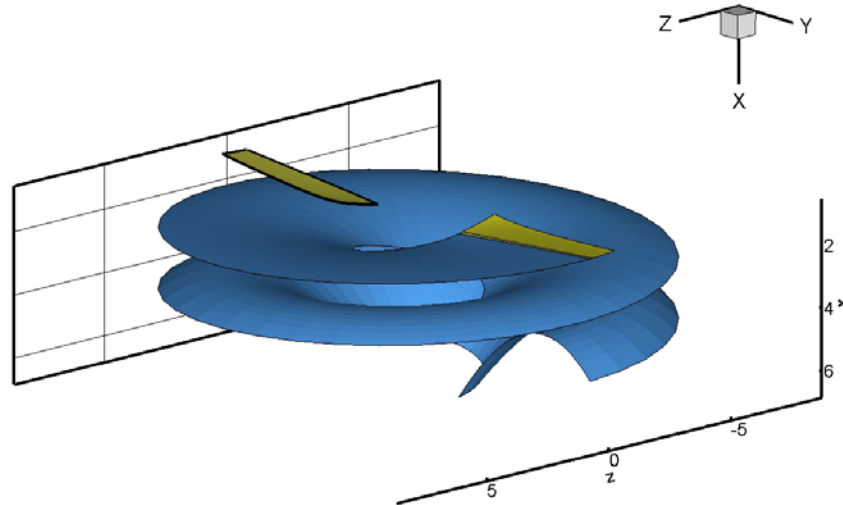


Figure 4: Wake from one blade of a two bladed wind turbine optimized for 9m/s with a square root angle of attack function

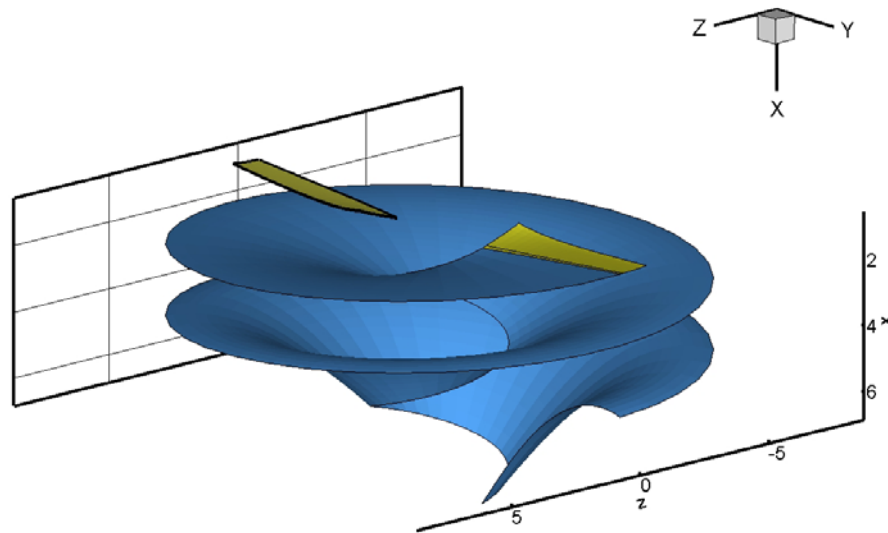


Figure 5: Wake from one blade of a two bladed wind turbine optimized for 12m/s with a square root angle of attack function

### Large Diameter Wind Turbine Optimization: Case 1

To further demonstrate the practicality of optimizing aerodynamic shapes for horizontal axis wind turbines using the vortex lattice method coupled with a genetic algorithm, three additional cases involving larger scale wind turbines with lower operating speeds were considered. The designs are crafted to closely follow the geometry of the Nordex S70 series power generating wind turbines. The blade diameter for these wind turbines is 70 m, the root chord is approximately 4 meters and the tip chord is 1-2 meters. The operating speed ranges up to approximately 20 rpm. The exact details for the air foil geometry are sketchy; however, this information is adequate to optimize the blade geometry for this class of wind turbines. The GA parameters were set to consider blade chord lengths in this range, a range of elliptic sweep distributions and a range of elliptic angle of attack functions. For the first case, a single point optimization (for power out) for a 10 m/s wind speed was performed assuming a wind turbine operating speed of 20 rpm. The GA was given a choice between 2 or 3 blades and chose the 3 blade option. 100 members were placed in the population for this case and the GA was set to run for 200 generations. A completely fixed blade geometry is thus assembled for the analysis. The resulting performance is compared to the Nordex machine in Figure 6. The agreement between the optimized machine and the Nordex machine is striking for the operating range of the Nordex machine. The higher wind speeds shown on the plot are rare and not likely to be optimized for and it is important to note that, in this higher speed area, the compressibility and viscous effects will cause the power curve to drop significantly below this more ideal operating curve. However, it would be expected that an inviscid, incompressible analysis of an optimized design would exceed the performance of a real operating wind turbine. Part of the reason for why this is not occurring is likely to be related to the wake distribution to be discussed in more detail later in the results section.

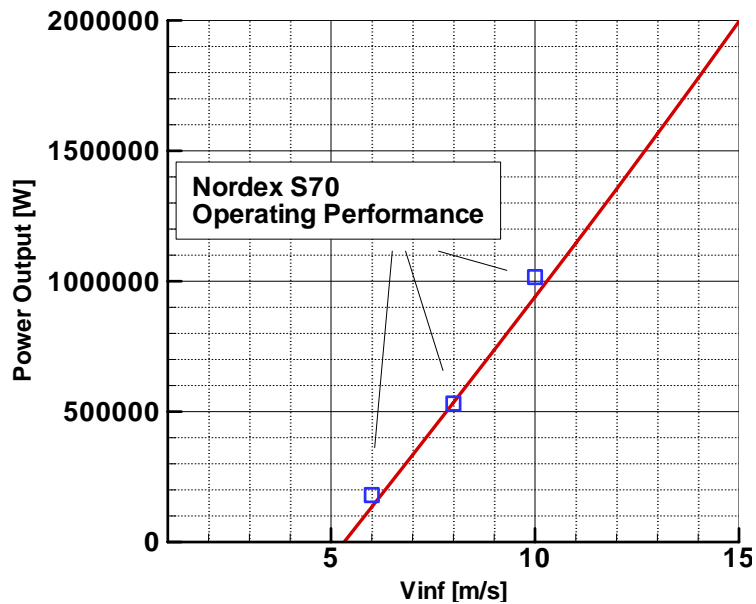


Figure 6: Power as function of wind speed for a 70 m wind turbine operating at 20 rpm with an elliptic angle of attack distribution.

The efficiency of the optimized wind turbine for case 1 is shown in Figure 7. Again, the efficiency peaks at a slightly lower wind speed than the speed at which power was maximized. The other noteworthy characteristic is that the efficiency curve has a rather sharp peak due probably at least in part to the fact that this is a single point optimization.

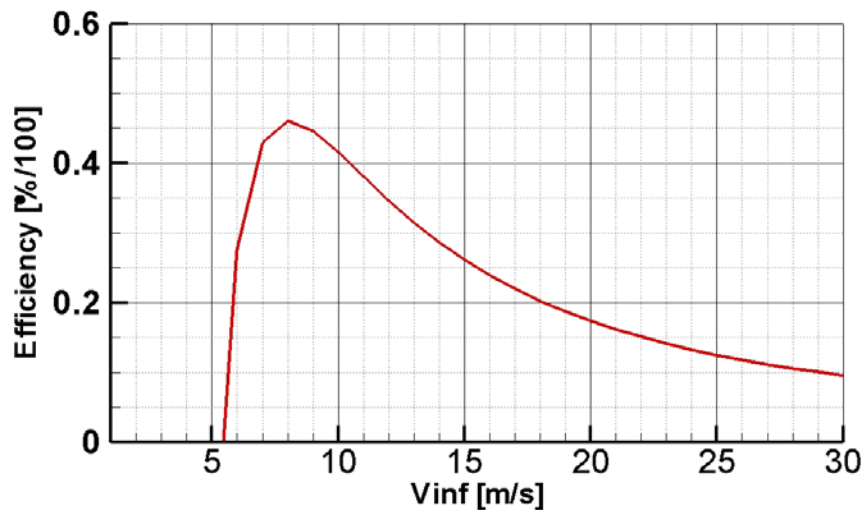


Figure 7: Efficiency for the single point optimization of a 70 m wind turbine at 10 m/s

The wake behavior is qualitatively characterized in the trailing legs plots shown in Figures 8 and 9. For Figure 8, the wake for only one of the three blades is shown for clarity. The angle of attack distribution for this analysis is the elliptic function. It is clear from Figure 8 that the blades are slowing the flow at about the  $\frac{3}{4}$  span location much more than at the hub or tip. From energy principles, it can be argued that a more uniform

distribution would be more efficient, hence a square root function is being implemented for this configuration.

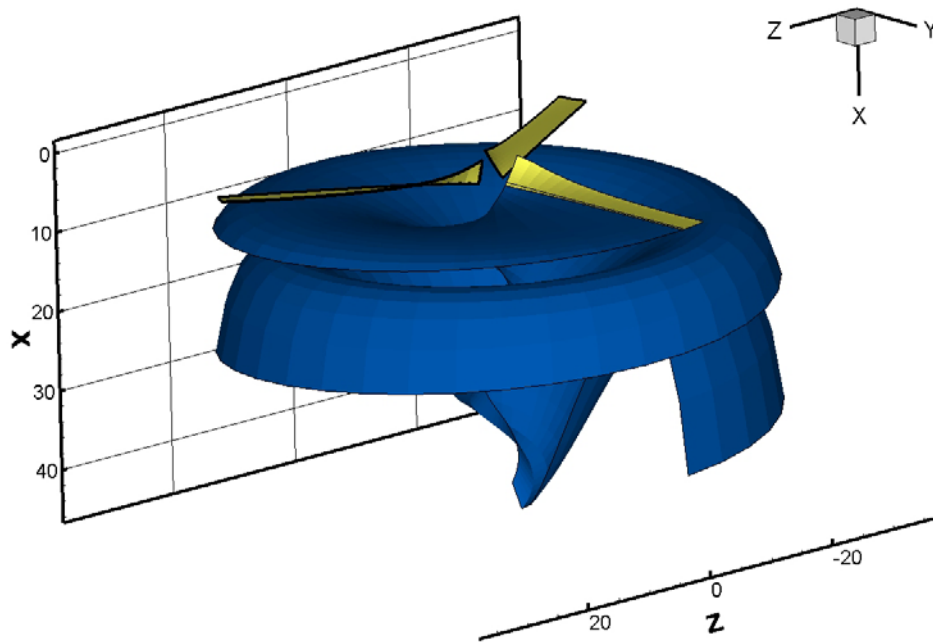


Figure 8: Wake from a single blade for the advance ratio optimization for a 70 meter diameter machine.

Figure 9 is included only to illustrate the intertwining of the wakes of the multiple rotors. The profile of the wake is less obvious but the illustration of the stacking of the blade wakes is instructive.

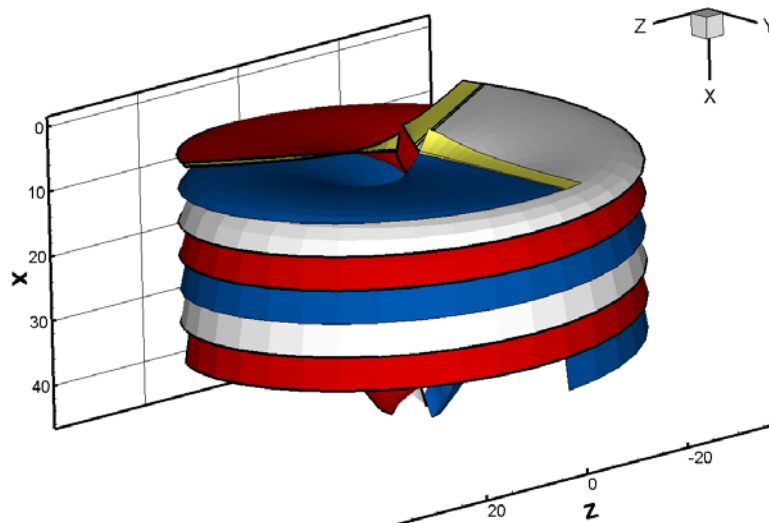


Figure 9: Wake from all three blades for case 1.

To illustrate the optimization process for the wind turbine, a plot of the figure of merit, power in this case, as a function of the generation is included in Figure 10. The

analysis program was originally developed for a propeller so the sign convention is that power out is negative. (This is opposite the traditional thermodynamic convention for systems but it is convenient for this analysis.) To maximize power out, the GA was set to minimize power in, thus the large negative numbers for the best performer. After approximately 125 generations, the performance improvement declines to a very low level indicating a high level of confidence in the convergence of the optimization.

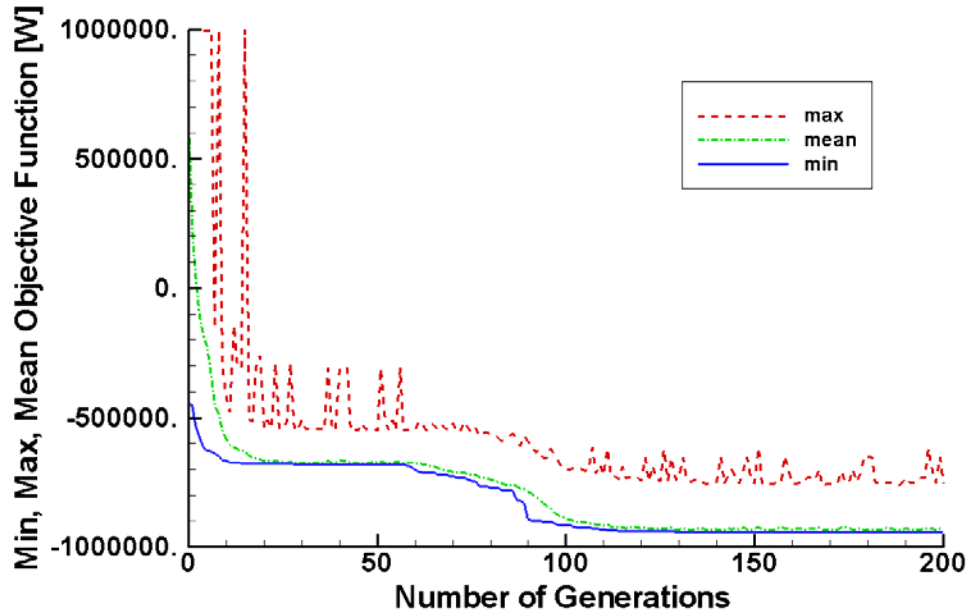


Figure 9: Performance of the population for the single point 70 m turbine optimization

### Large Diameter Wind Turbine Optimizations: Case 2

Single point optimizations are certainly valuable and instructive but, in practice, wind turbines spend most of their lives away from any single design point. The approach taken in this effort is to select a primary advance ratio (6 m/s) for this case, fix the geometry for this advance ratio and angle of attack distribution, and then, for the “off-design” condition, rotate the entire fixed geometry through a GA determined pitch angle change and then rerun this geometry for the “off-design” wind speed (10 m/s in this case). For case 2, two operating speeds were selected and the performance for these two operating conditions was weighted according to the Weibul distribution. 150 members, 120 generations were selected for this case. Otherwise, the GA was set exactly as for case 1. The performance of the resulting wind turbine is characterized by the power distribution function shown in Figure 10 and the efficiency distribution shown in Figure 11. These curves are calculated for fixed geometries and fixed pitch angles. The optimum operating condition would obviously correspond to a continuously varying pitch angle but the curves are shown primarily to illustrate the overall characteristics of the performance and not the true operating conditions. An optimized operating profile could be generated by the GA as a part of the preliminary design process.

The performance behavior for the 10 m/s case is similar to the single point optimization performance but the performance at 6 m/s is slightly improved. The efficiency of the machine at the lower speeds is at least slightly over predicted in this case since the efficiency exceeds the Betz limit.

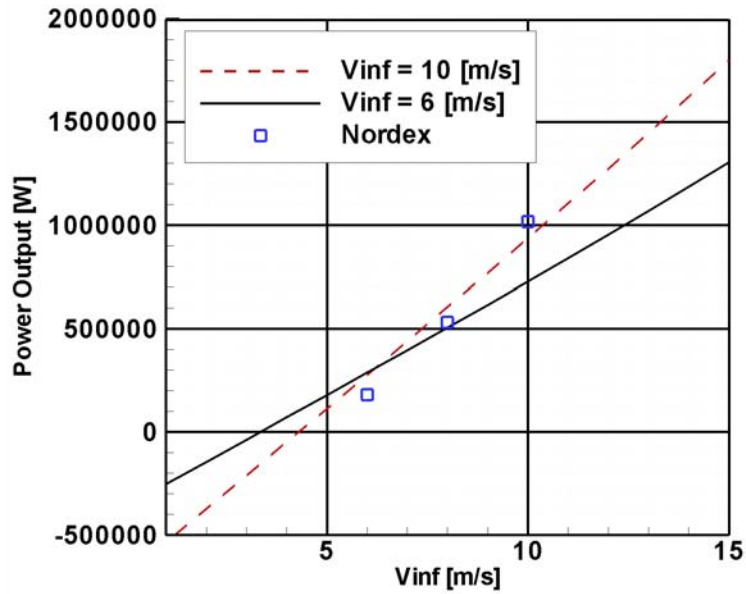


Figure 10: Power output for case 2

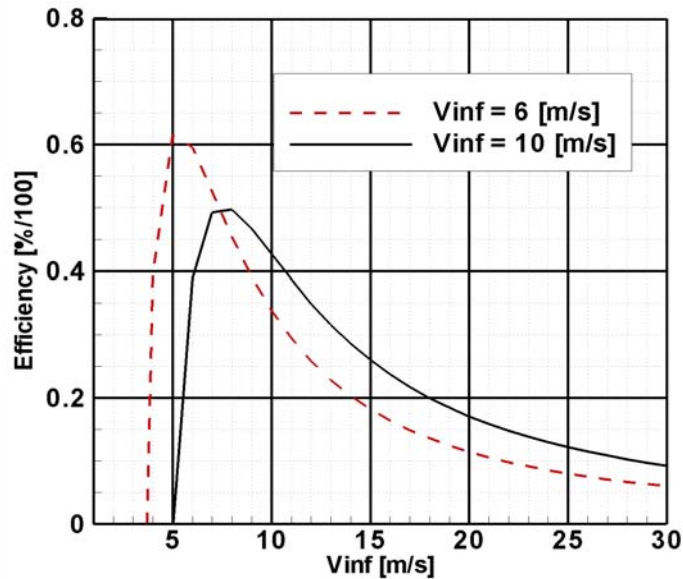


Figure 11: Efficiency of fixed pitch bladed 70 m wind turbine.

The elliptic angle of attack functions associated with the 6 m/s design point and the offset distribution for the 10 m/s operating condition are shown in Figure 12. The GA determined pitch change for the entire fixed geometry blade is approximately 3.2 degrees. This twist results in a change in the true angle of attack for the airfoil that depends on the radial location. The change is much more dramatic near the hub than at the tip and would likely result in separation near the hub. Alternative procedures such as designing the blade initially for the higher operating speed and then rotating for the lower operating speeds are now being investigated.

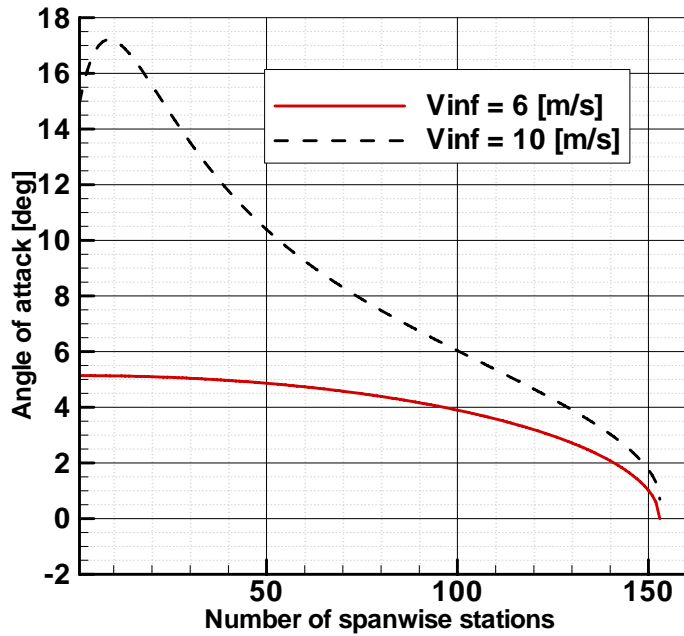


Figure 12: True Angle of attack distribution for case 2.

The wake behavior for this design is characterized in Figures 13 and 14. Since an elliptic distribution is assumed for the angle of attack function, the character of the wake is not markedly different from case 1. Because of the higher free stream velocity, the wake in Figure 14 is stretched out further but is nearly identical to the wake in Figure 13 otherwise.

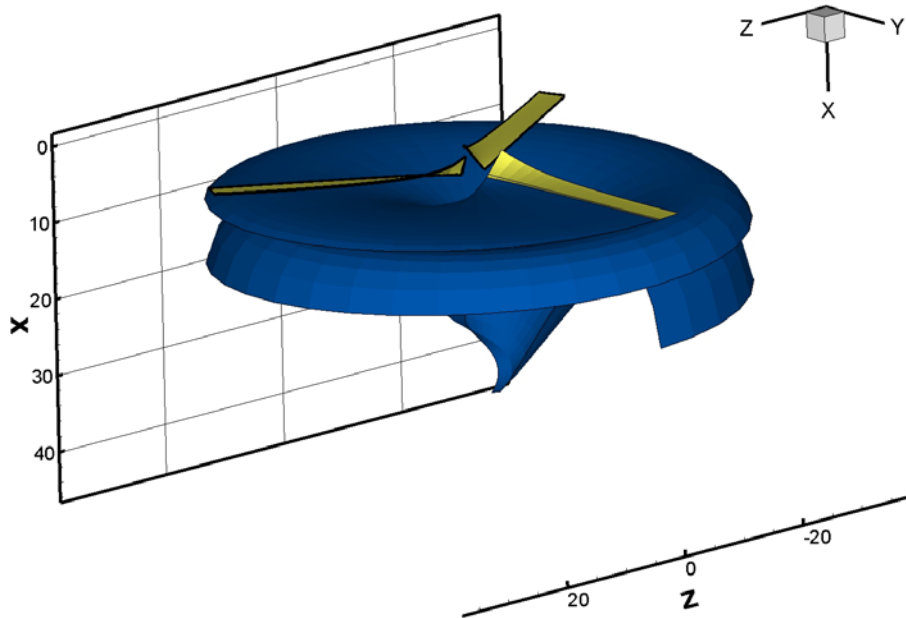


Figure 13: Wake for the 6 m/s operating condition for case 2

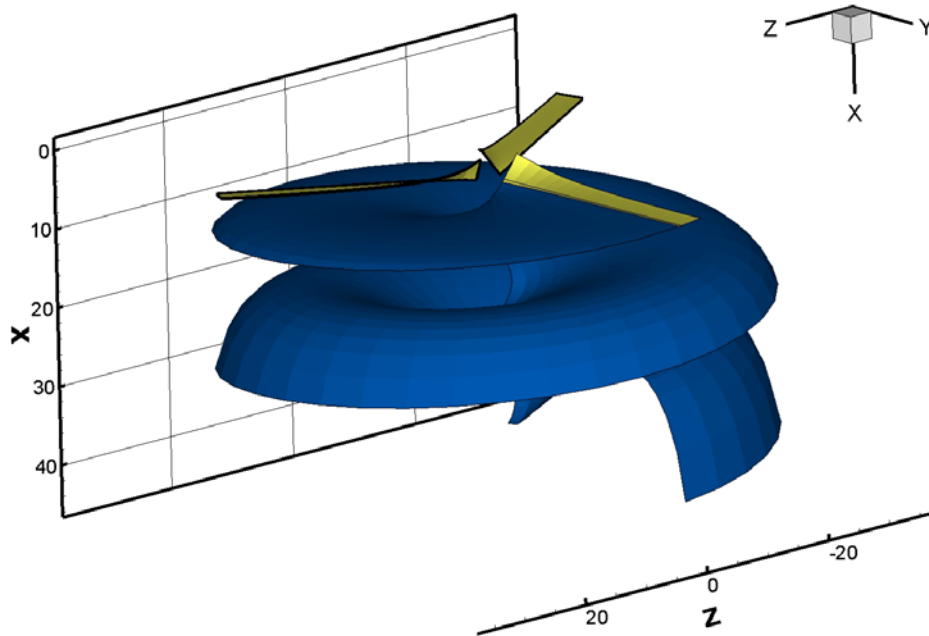


Figure 14: Wake for the 10 m/s operating condition for case 2.

### Large Diameter Wind Turbine Optimizations: Case 3

For case 3, three operating speeds were selected and the performance for these three operating conditions was again weighted according to the Weibull distribution. 150 members, 160 generations were selected for this case. Otherwise, the GA was set exactly as for case 2. The performance of the resulting wind turbine is characterized by the power distribution function shown in Figure 15 and the efficiency distribution shown in Figure 16. Again, these curves are calculated for fixed geometries and fixed pitch angles and are shown primarily to illustrate the overall characteristics of the performance rather than the true operating conditions.

The performance behavior for the 10 m/s case is again similar to the single point optimization performance but the performances at 6 m/s and 8 m/s are slightly improved as might be expected in a multipoint optimization. Again, the efficiency of the machine at the lower speeds is at least slightly over predicted in this case since the efficiency again slightly exceeds the Betz limit.

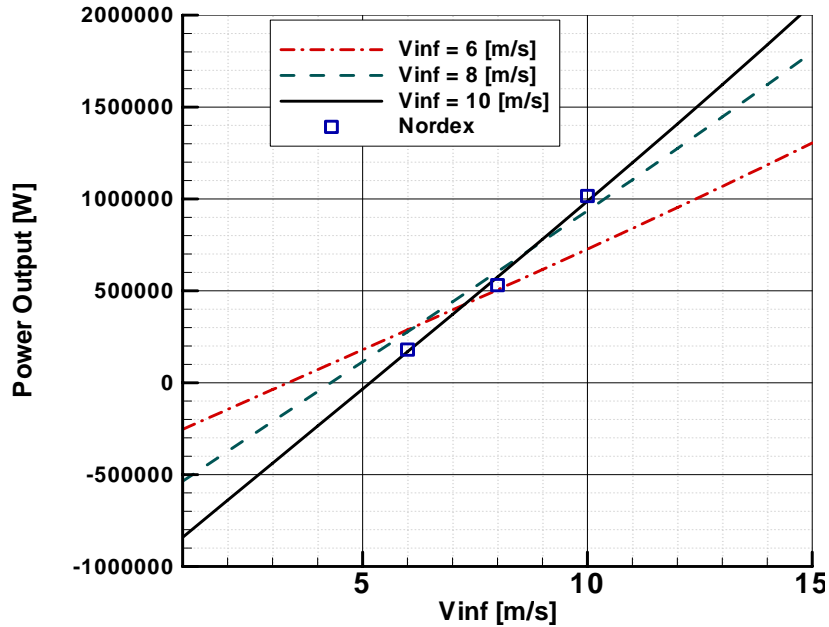


Figure 15: Power output for case 3.

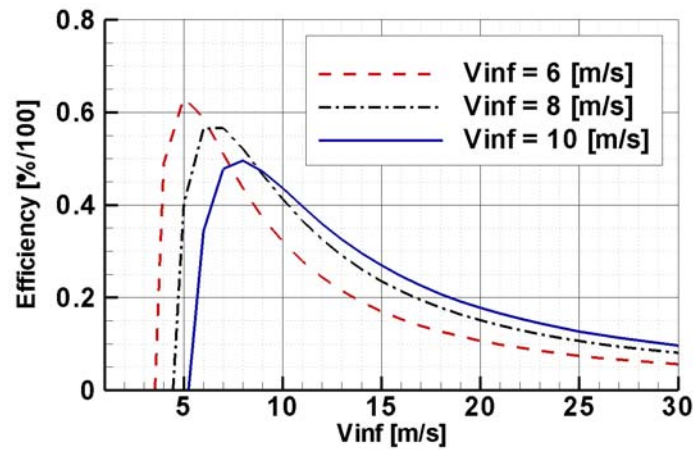


Figure 16: Efficiency for case 3

The elliptic angle of attack distribution is depicted in Figure 17. In this case as in the other elliptic distributions, the optimum distribution at the 6 m/s is nearly fully elliptic when only elliptic angle of attack distribution functions are considered. The pitch change between the 6 and 10 m/s cases is almost the same and the pitch change for the 8 m/s case is approximately 2 degrees from the 6 m/s case. Again, the true angle of attack steepens near the hub but goes to near zero at the tip in all cases. The wake characteristics for this case are not shown but were found to be essentially identical in overall appearance to those shown above for the elliptic distributions.

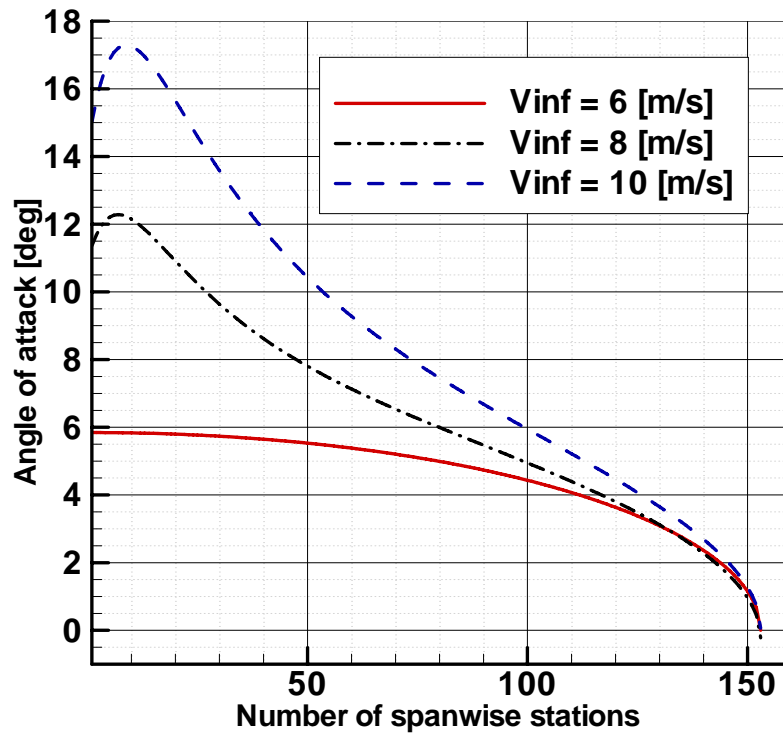


Figure 17: True angle of attack for case 3

### Comparison between elliptic and parabolic angle of attack functions

If the Betz argument is taken piecemeal in a radially outward direction, it can be argued that a more uniform wake might lead to more efficient wind turbines. This has turned out to be the case in propeller optimization efforts. The elliptic distributions for angle of attack considered above clearly will not allow for the more uniform wakes for constant camber airfoils in the wind turbine case. In an effort to address this consideration, a parabolic distribution used in the small diameter wind turbine analysis above was implemented and compared to the elliptic distribution for the large diameter wind turbine.

The particulars of the case considered for this comparison involved a 10 m/s wind, a 70 m diameter wind turbine and an operating speed of 19 rpm. Substantial flexibility was given to the GA to determine the parameters for the optimum shape for the angle of attack function. 150 members were placed in the population and the GA was run through 150 generations for the two cases. Convergence was not clearly demonstrated for these two cases but the changes in the objective function (power output) were small near the end of these runs. The resulting angle of attack distributions are compared in Figure 18. Momentum/energy arguments could be used to explain the distribution of the chosen for the parabolic function; however, the overall performance of the wind turbine did not substantially change as can be seen in Figures 19 and 20. Clearly, the use of a more universal angle of attack function would be of interest.

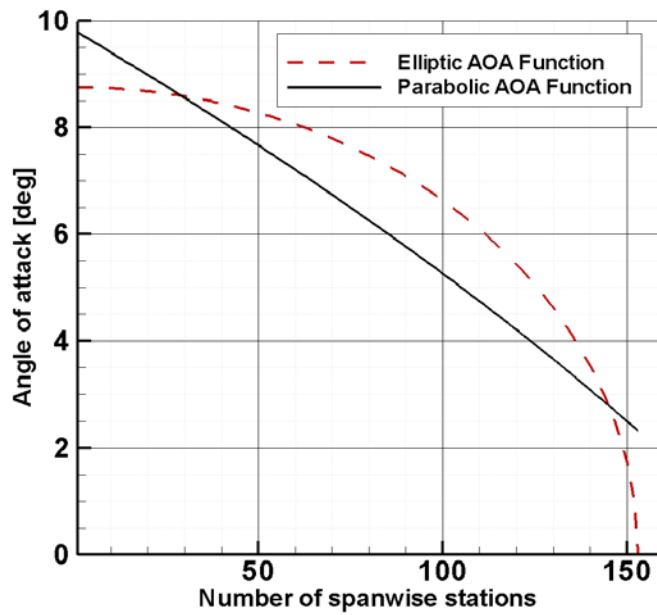


Figure 18: Angle of Attack distribution comparison

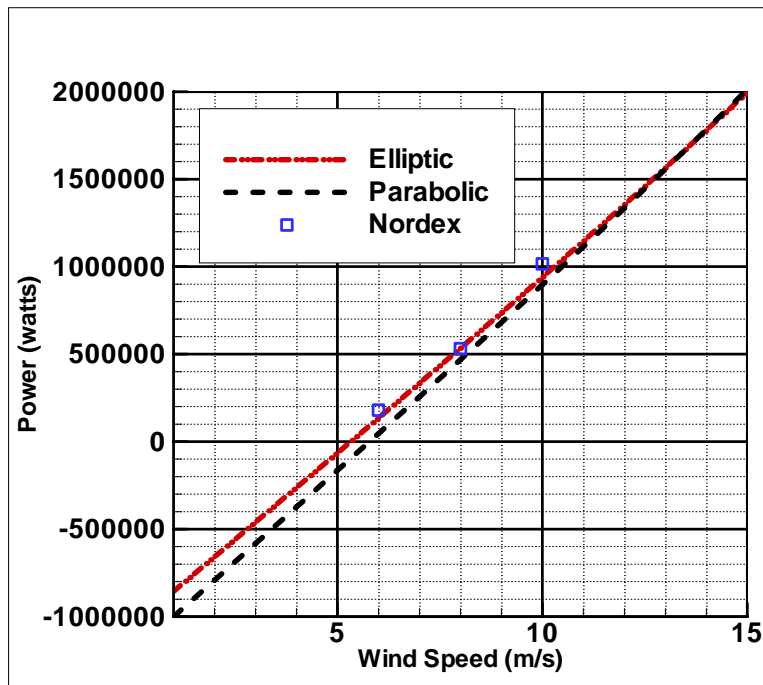


Figure 19: Power comparison for angle of attack distributions

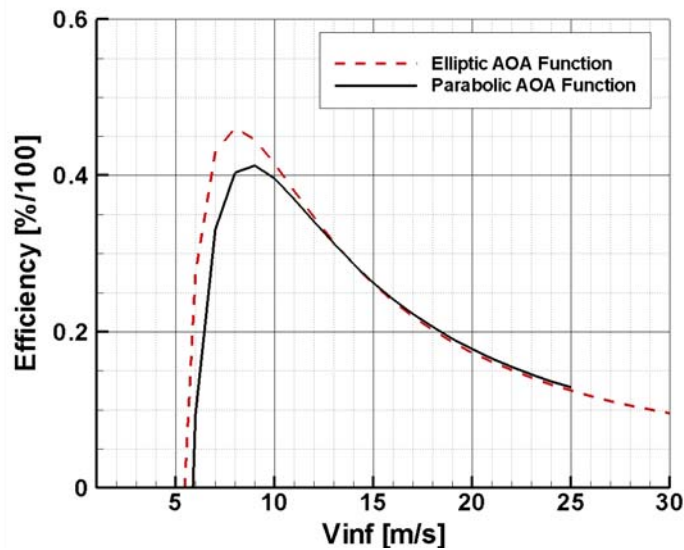


Figure 20: Comparison between elliptic and parabolic angle of attack functions.

To illustrate the differences in the character of the wake between the elliptic and parabolic angle of attack functions, the wake for the parabolic distribution is shown in Figure 21. The peak flow retardation point has moved outward along the blade as might be expected by looking at the angle of attack distributions considering the rotation of the blades but the near hub area and the tip areas are retarded much less than the central portion in both cases.

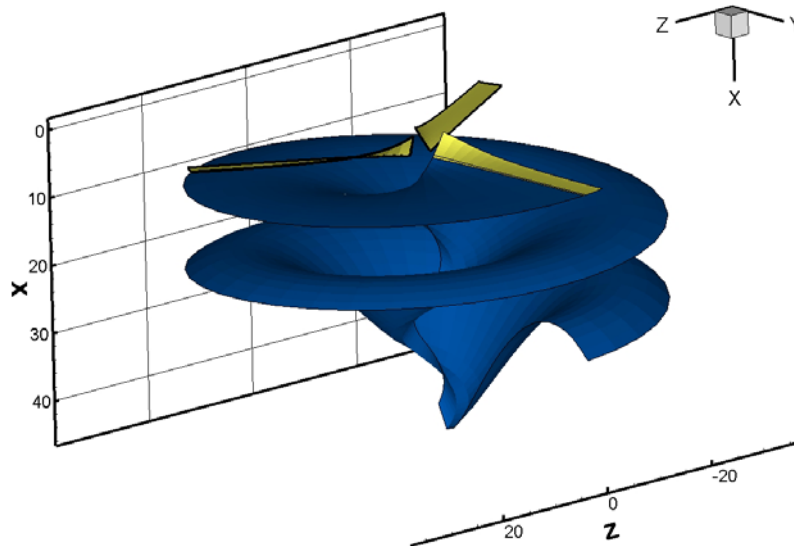


Figure 21: Wake from a 70 m wind turbine optimized for a 19 rpm, 10 m/s condition.

### Conclusions and Future Work

With this work, it has been shown that the performance of horizontal axis wind turbines can be accurately and efficiently modeled using the vortex lattice method. It has also been shown that this prediction scheme is viable as a prediction tool used in a Genetic

Algorithm based optimization process. This effort clearly represents the first step toward generating a multidisciplinary optimization scheme which would allow the entire wind turbine to be optimized simultaneously including the aerodynamic shapes, the structure and the power plant. It would be of significant interest to consider variable shaped blades devised using active materials and other state of the art technologies in the optimization process. The inclusion of an economics model to optimize the total economic performance of horizontal axis wind turbine installations would also be a logical and highly desirable extension.

Aerodynamically, the design modeling and flexibility could be improved by adding variably cambered airfoils, a more comprehensive approach to modeling the wake, two layered vortex lattice modeling to account for thick airfoils, compressibility, a model to account for viscous effects, and more flexibility in the angle of attack function.

### References

1. Hampsey, M., 2002, "Multiobjective Evolutionary Optimisation of Small Wind Turbine Blades," PhD Dissertation, University of Newcastle.
2. Glauert, H., 1935, "Airplane Propellers," *Aerodynamic Theory*, ed, W. F. Durand, Julius Springer, Berlin, pp. 169-360.
3. Wilson, R. E., Lissaman, P. B. S., and Walker, S. N., 1976, "Aerodynamic Performance of Wind Turbines," Department of Mechanical Engineering, Oregon State University, Corvallis, Oregon, National Science Foundation, Research Applied to National Needs, (RANN), Rep. No. NSF/RA-760228, NTIS PB 238594, June.
4. Ostowari, C, and Naik, D., 1984, "Post Stall Studies of Untwisted Varying Aspect Ratio Blades with a NACA 4415 AirFoil Section-Part I," *Wind Engineering*, Vol. 8, No. 3, pp. 176-194..
5. Ostowari, C, and Naik, D., 1985, "Post Stall Studies of Untwisted Varying Aspect Ratio Blades with a NACA 44XX AirFoil Section-Part II," *Wind Engineering*, Vol. 9, No. 3, pp. 149-164.
6. Selig, M. S., and Coverstone-Carroll, V. L., 1996, "Application of a Genetic Algorithm to Wind Turbine Design," *Journal of Energy Resources Technology*, Vol. 118, March 1996, pp. 22-28.
7. Fiddes, S. P., and Gaydon, J. H., 1996, "A New Vortex Lattice Method for Calculating the Flow Past Yacht Sails," *Journal of Wind Engineering*, Vol. 63, pp. 35-59.
8. Anders Smaerup Olsen, "*Optimization of Propellers using the Vortex Lattice Method*", Technical University of Denmark, Dec 2001.
9. Burger, Christoph and Hartfield, Roy J., "Propeller Performance Optimization using Vortex Lattice Theory and a Genetic Algorithm", AIAA-2006-1067, presented at the 44th Aerospace Sciences Meeting and Exhibit, Reno, NV, Jan 9-12, 2006.
10. Shiu Wing Cheung, R. "Numerical Prediction of Propeller Performance by Vortex Lattice Method", *UTIAS Technical Note No.265 Nov 1987*.
11. Anderson, M. B., Burkhalter, J. E. and Jenkins, R. M., "Design of a Guided Missile Interceptor Using Genetic Algorithms", *Journal of Spacecraft and Rockets*, Vol 38, No.1, Jan. 2001.

12. Anderson, M. B., Burkhalter, J. E. and Jenkins, R. M., "Missile Performance Optimization Using Pareto Genetic Algorithms", *AIAA 99-0261, 37<sup>th</sup> AIAA Aerospace Science Conference, Reno NV, Jan 1999.*
13. James R. M., "*On the remarkable Accuracy of the Vortex Lattice Method*", *Computer Methods in Applied Mechanics and Engineering*, 1:59-79, 1972
14. John J. Bertin, and Michael L. Smith, *Aerodynamic for Engineers, 2<sup>nd</sup>ed.*, Prentice Hall, Englewood Cliffs, New Jersey, 1989.
15. Katz, Joseph and Plotkin, Allen, *Low-Speed Aerodynamics From Wing Theory to Panel Methods*, McGraw-Hill, New York, 1991.
16. Goldstein, S., "*On the Vortex Theory of Screw Propellers*", *Proceedings of the Royal Society of London, Series A, Vol. 123, 1929*
17. Eppler, Richard and Hepperle, Martin, "A procedure for Propeller Design by Inverse Methods," *G.S. Dulikravich proceedings of the International Conference on Inverse Design Concepts in Engineering Sciences (ICIDES)*, pp. 445-460, Austin, TX, October 17-18, 1984.